NASA Technical Memorandum 82983

STIF

Technology and Benefits of Aircraft Counter Rotation Propellers

W. C. Strack and G. Knip
Lewis Research Center
Cleveland, Ohio

and

A. L. Weisbrich
Hamilton Standard
Windsor Locks, Connecticut

and

J. Godston
Pratt & Whitney
East Hartford, Connecticut

and

E. Bradley
Lockheed-Georgia Company
Marietta, Georgia

Prepared for the
1982 Aerospace Congress and Exposition
sponsored by the Society of Automotive Engineers
Anaheim, California, October 25-28, 1982

ERRATA

NASA Technical Memorandum 82983

TECHNOLOGY AND BENEFITS OF AIRCRAFT COUNTER ROTATION PROPELLERS

W. C. Strack, G. Knip, A. L. Weisbrich, J. Godston,
and E. Bradley
October 1982

Tables III and IV should be replaced with the attached tables.

Figures 21, 23, and 24 should be replaced with the attached figures.

TECHNOLOGY AND BENEFITS OF AIRCRAFT COUNTER ROTATION PROPELLERS

W. C. Strack and G. Knip
NASA Lewis Research Center
Cleveland, Ohio
and
A. L. Weisbrich
Hamilton-Standard
Windsor Locks, Connecticut
and
J. Godston
Pratt & Whitney
East Hartford, Connecticut
and
E. Bradley
Lockheed-Georgia Company
Marietta, Georgia

ABSTRACT

Results are reported of a NASA sponsored analytical investigation into the merits of advanced counter rotation propellers for Mach 0.80 commercial transport application. The study considered propeller and gearbox performance, acoustics, vibration characteristics, weight, cost and maintenance requirements for a variety of design parameters and special features. Fuel savings in the neighborhood of 8 percent relative to single rotation configurations are feasible through swirl recovery and lighter gearboxes. This is the net gain wh ch includes a 5 percent acoustic treatment weight penalty to offset the broader frequency spectrum of the noise produced by counter rotation propellers.

IN 1975, NASA-LEWIS INITIATED a research program addressing high speed propeller technology. Since then, the emergence of the prop-fan as a fuel conservative competitor to the high pressure ratio turbofan has created new interest in propeller technology development. Both the analytical studies and wind tunnel tests have shown that efficiencies of about 80 percent are achievable at the flight Mach number region of 0.7 to 0.8 where single rotation prop-fans (SRP) are intended for operation. Although the prop-fan is lightly loaded in relation to a high pressure ratio turbofan, it is highly loaded in relation to today's three and four bladed propellers designed for lower flight speeds. Loadings expressed as shaft horsepower divided by the square of the blade tip diameter, SHP/D^2, at their cruise design point are about 300 for a 1.60 pressure ratio turbofan, 30 to 40 for prop-fans and 10 to 15 for low-speed application three and four bladed propellers. The turbofan has the smallest diameter and imparts the highest swirl velocity to the airstream. The swirl from the turbofan rotor is turned to the axial direction by a downstream row of stator blades. These stators convert the swirl to a static pressure rise which appears as an increase in propulsive thrust and yieids a cruise efficiency of about 65 percent. The lightly loaded three and four bladed propellers used in low-speed aircraft do not impart high swirl velocities and as a result do not have a significant amount of swirl energy in the slipstream. The single rotation prop-fan diameters are about 50 percent smaller than conventional propellers. Swirl velocities for the prop-fans are higher and full recovery of the swirl energy by employing counter rotation could improve the design point cruise efficiency by about 8 efficiency points. This potential for increased fuel savings was the main impetus of this study.

The present study was conducted at the 0.8 Mach number condition to allow comparison with available 0.8 Mach number SRP information. However, it is not intended to promulgate 0.8 Mach number counter rotation propeller (CRP) operation.

HISTORY OF COUNTER ROTATION

This potential has intrigued the designers of a variety of advanced, special purpose aircraft because of the possible large gains in mission performance. However, despite repeated attempts to apply counter rotation, such propellers have generally not proven viable because of their higher cost and lower reliability which have more than offset the benefits. Accordingly, only a relatively few limited production installations have gone into service in the United States. Examples of U.S. counter

rotation propeller aircraft are the Vought F4U, the Convair R3Y-1, and the Northrop XB-35, among others (fig. 1).

The one production usage in the United States was the Convair R3Y Navy flying boat powered by four 5000 hp Allison T-40 engines each driving a 15-foot diameter six-bladed counter rotation propeller. Eleven of these aircraft were built and were in operational service for several years beginning in 1954.

Successful examples of foreign counter rotation designs are the Russian TU-114 commercial transport (fig. 2) which have been in operational service for over 20 years and apparently have been performing effective missions.

Another, less publicized production application of counter rotation propellers is the British Avro "Shackleton" 4-engine reconnaissance aircraft. This aircraft was first flown in early 1949 and there are still approximately 200 aircraft in the South African Air Force. This installation has 4 Rolls-Royce Griffon 57 piston engines rated at 2450 hp, each driving a de Havilland 6-bladed, 13.0-foot diameter propeller.

COUNTER ROTATION COMPLICATIONS - It should be noted that in the cited historical aircraft, use of the counter rotation propeller and gearbox involved radical departures from previous design practices. In some cases the resulting designs added considerable complexity and weight to the propeller system (fig. 3). The subsequent result was greater cost and maintenance requirements. Also, aircraft programs of that time did not allow for sufficient component development in critical areas such as oil seals, pumps, hydraulic motors, gear trains, bearings, etc. This lack of development resulted in a myriad of operational problems ranging from internal and external leakages to actual gear train failures. It was this adverse operational experience, more than hardware costs, that discouraged the further use of counter rotation in the past.

In retrospect, it is clear that these prior attempts to introduce counter rotation propellers were severely handicapped by two factors: a lack of refinement in the appropriate technologies, and insufficient hardware development. Furthermore, they did not involve sufficiently stringent design conditions (aircraft speed, propeller disk loading, etc.) to attain the full potential of counter rotation.

None of these problems represented fundamental deficiencies of the counter rotation concept, and all were amendable to effective solution given proper development effort. However, the strong post-war move toward jet propulsion reduced propeller development and the available propeller R&D funding was concentrated on the development of the single rotation turboprop. Many of the mechanical design refinements that emerged from the single rotation turboprop programs could have been equally effective for counter rotation, but came too late to revive an interest.

It was also recognized that the aerodynamic and acoustic analysis methods for counter rotation had not been fully developed and would require further significant effort to bring them to an adequate level of refinement for production usage. A major improvement to the aerodynamic methodology was made by T. Theodorsen of NACA in the mid 1950's, and was applied to the aerodynamic design of several successful, experimental counter rotation propellers. Current aerodynamic and acoustic prediction methodology has been developed for high speed counter rotation prop-fans which is a significant extension of previous analytical capability.

Any future counter rotation prop-fans would presumably still be faced with added design complexity, weight and costs. The main objective of the NASA sponsored study reported here was to determine whether the performance benefits of a properly designed counter rotation prop-fan/gearbox combination would substantially offset these disadvantages.

HISTORICAL PERFORMANCE DATA - Based on previous SBAC prediction methods (1)*, variations in ideal efficiency with tip speed and power loading for single and counter rotation, 10-bladed propellers are shown in figure 4 for 0.80 Mach cruise at an altitude of 35000 feet. Experience has shown that single rotation propellers can achieve actual efficiency levels within about 4 percentage units of those shown.

Swirl recovery reduces the magnitude of efficiency degradations at high power loadings and/or low tip speeds typically associated with single rotation propellers. Therefore, the ideal efficiency advantage offered by counter rotation propellers varies from about 5 to 15 units of efficiency for the range of conditions shown in figure 4.

*Numbers in parenthesis designate References at end of paper.

A literature survey has shown that the comparative performance levels between single and counter rotation propellers have also been established experimentally using models. The model propellers were predominately low speed designs in that the blades were fairly thick and unswept. When these models were tested at high Mach numbers, 0.80 for instance, both the single and counter rotation propellers exhibited low efficiency levels at tip speeds and power loadings corresponding to prop-fans. However, the trends nearly always showed that the counter rotation propeller efficiencies were significantly higher than those for the single rotation propellers. The tabulation of experimental efficiency gains in Table 1 shows the eight-bladed counter rotation efficiencies to be 11 units higher than for the single rotation propellers (2). These are based upon low Mach number test results at advance ratios and power coefficients that simulate the tip speeds and power loadings appropriate for 0.80 Mach cruise at an altitude of 35,000 feet. The experimental gains are shown to exceed the ideal efficiency gains by about 2 1/2 percentage points, a trend fairly typical of the early model test results and is probably due to the relatively poor performance of the single rotation propellers.

PROPELLER PARAMETRIC ANALYSIS

BASELINE PROPELLER DEFINITION - Using modern computational techniques for determining aerodynamic performance, acoustics, and weight, a parametric analysis of counter rotation propellers (CRP) was performed to produce a preliminary CRP design at a typical Mach 0.8/35000 foot cruise altitude that minimized mission fuel for a commercial transport. This process began with the specification of the baseline CRP parameter values displayed in Table 2 which were selected on judgment alone. This baseline has a blade geometry similar to the 10-bladed SR-7 single rotation prop-fan (SRP) which is being designed and fabricated as a technology verification effort. The ten blades were divided five to a disc and the three quarter radius front and rear disc blade angles were set appropriately to absorb the same power at equal tip speeds. The blade twists were modified to maximize efficiency and to have equal torques at each blade element. In addition, the blade activity factor (AF) and camber were varied to maximize efficiency for the inflow into the counter rotation propellers. As a result, the blade widths were narrowed by about 6 percent relative to the SR propeller to an activity factor of 180 per blade, and the camber (integrated design lift coefficient) was increased from 0.21 to 0.31.

AERODYNAMIC PERFORMANCE - Using a single average cruise point analysis and this baseline geometry, cruise efficiency variations with power loading and tip speed were determined as shown in figure 5. The peak efficiency is slightly higher than 89 percent and occurs at about 700 feet per second tip speed and somewhat higher power loading than the 32 SHP/D^2 baseline. Efficiency is not strongly affected by power loading as indicated previously by the ideal efficiency curves (fig. 4). The comparatively low efficiency level at 600 feet per second tip speed is partially due to the non-optimum baseline geometry for such a low speed. It is reasonable to expect an efficiency improvement for a dedicated low tip speed design by raising solidity, raising camber, and retwisting. For example, a side calculation with 50 percent more solidity at 35 SHP/D^2 produced a 0.6 percent efficiency improvement. Nevertheless, the added weight associated with the increased solidity more than offset the cruise efficiency improvement. Furthermore, low tip speeds adversely affect takeoff performance too.

WEIGHT TRENDS - The weights of the propellers, gearboxes, landing gear, and fuselage acoustic treatment are all affected by the propeller power loading and tip speed. Hence the weight of each of these subsystems was determined to enable performance versus weight tradeoffs to be included in the overall selection of CR propeller parameters.

Weight trends for two counter rotation propeller systems, including blades, spinner, pitch change system and disk without tailshaft, are shown at the left of figure 6. Propeller weights are shown to decrease with increasing power loading (decreasing diameter) and decreasing tip speed. Generalized gearbox weight trends, shown in the center of the figure, are similarly affected by power loading but inversely affected by the lower torques of the higher tip speeds. The effect of power loading on the landing gear weight of a low-wing airplane is shown by the curve at the right in figure 6. The smaller propeller diameter resulting from increasing power loading results in lower landing gear weights. These data were calculated from information provided by the Lockheed-California Company and reference (3).

From the estimated near-field noise levels at the fuselage, shown on the left of figure 7, (discussed later) the required fuselage treatment weight to attain 82 dBA cabin noise level was calculated as a function of tip speed and power loading as shown on the right. It can be seen that minimum treatment weight is obtained with the lowest tip speed because exterior noise is

minimized. Also, if operation at higher tip speeds is selected, then acoustic treatment weight is minimized at high cruise power loading. This trend is caused by the increased tip clearance at higher power loadings and resulting lower fuselage sidewall noise. The equations used to calculate each of the subsystem weights are listed in the appendix.

The total relative CRP weight trend is shown in figure 8. This includes two baseline counter rotation propellers, two gearboxes, the landing gear and fuselage acoustic treatment. The weights are relative to the baseline power loading of 32 SHP/D^2 and tip speed of 700 feet per second. Since all four components become lighter with increased power loading, the total weight does also. High tip speeds favor lighter weight gearboxes but the reverse trend for the propeller assembly and acoustic treatment combine to drive the selection toward lower tip speeds.

PARAMETER SELECTION - The foregoing propeller efficiency and total system weight data were used together with sensitivity trade factors to determine the power loading and tip speed that minimize mission fuel. The trade factors were generated by Lockheed-Georgia for a 100 passenger, Mach 0.8 twin engine transport powered by single rotation prop-fans: 1.0 percent fuel burned difference results from either a 0.8 percent change in propeller efficiency or a 790 pound total weight change. The resulting fuel burned curves (fig 9) show that somewhat higher power loading and tip speed are desirable relative to the original baseline values. A power loading of about 37 HP/D^2 and a tip speed of 750 ft/sec result in about a 1 percent fuel improvement.

Using these power loading and tip speed values, additional investigations were performed of several secondary variables; namely, the number of blades, blade sweep, spacing between the front and rear propeller disks, nacelle-to-propeller diameter ratio, front-to-rear tip speed ratio, and front-to-rear propeller diameter ratio. The effects of these geometric variables on fuel burned, cruise efficiency, and component weights are shown in figure 10.

The effects caused by varying the number of blades relative to the baseline CRP are shown in figure 10(a) and indicate fuel burned is reduced with increasing number of blades. The solid lines in the figure connect 8, 10, and 12-bladed configurations having the same total activity factor (the product of activity factor per blade and number of blades). Relative to the 10-bladed baseline, the blade chords are wider with eight blades and narrower with twelve blades. Cruise efficiency and acoustic treatment weight are significantly improved for 12-blades and fuel burned is down 2 percent. However, blade design practice has shown that the narrow chords of a 12-bladed arrangement would require thickening to be structurally feasible. Thickening would adversely affect performance, and to circumvent this an alternative configuration was analyzed having twelve baseline blades--total activity factor increased 20 percent, from 1800 to 2160. This configuration, shown by the open-circle symbols in figure 10(a), also adversely affects efficiency, propeller weight, and acoustic treatment weight, but fuel burned is still 0.9 percent lower than the baseline 10-bladed CRP.

Single rotation prop-fans have demonstrated that incorporating blade sweep has the effect of improving efficiency and reducing noise at cruise. This trend was also found to be true in the CRP parametric study as is shown in figure 10(b). Both cruise efficiency and acoustic treatment weight are quite adversely affected as tip sweep is reduced below the 40^{o} baseline sweep. The straight bladed configuration requires about 3600 pounds of additional acoustic treatment and its cruise efficiency is down by more than 6 percent. These are the principal contributors to the 12 percent increase in fuel burned for the unswept CRP. Careful attention to design details has shown that the efficiency decrement for an unswept SR prop-fan can be maintained at about 3 percent. Similar penalty alleviation is expected to be possible for the unswept counter rotation propeller. Propeller sweep angles greater than about 45^{o} result in increased blade structural limitations.

Sweeping the blades forward rather than rearward produced a 2 percent fuel reduction due to efficiency improvement. However, this trend was not anticipated and at this time is judged to need further investigation, both analytically and experimentally. Should forward sweep actually prove to provide a benefit, it should be noted that similar improvements would occcur for single rotation prop-fans.

Disk spacing is illustrated by the sketch on figure 10(c). Changes in fuel burned, cruise efficiency and component weights are shown for blade centerline spacing ranging from 18 percent to 36 percent of the CRP diameter. The plot indicates minimum fuel burned at minimum spacing. The smallest spacing represents the minimum practical clearance between the trailing edge of the front blades and the leading edge of the rear blades due to blade

pitch change. The effect of spacing on cruise efficiency is negligible and because the aerodynamic interaction noise is not an important noise source, spacing has little affect on the acoustic treatment weight required to reach the 82 dBA cabin noise objective. The only significant change for doubling spacing is a 1130 pound increase in gearbox weight related to shaft critical speed factor penalties. The gearbox weight increase together with the other minor changes in cruise efficiency, CRP weight and acoustic treatment weight, increase fuel burned by 1.3 percent.

Nacelles ranging in size from 25 to 35 percent of the propeller diameter were also investigated. This encompasses sizes typical of single rotation prop-fans (35 percent) and the smaller nacelles which are conceptually feasible for an inline CPR planetary gearbox. SR prop-fan nacelles are designed to minimize compressibility losses where the large diameter effectively reduces the local velocities in the propeller plane. The effect of this is to minimize compressibility losses, particularly the inboard blade row choke losses. Counter rotation propellers, which have large channel areas in both the front and rear blade rows, are less susceptible to choking losses.

The effect of nacelle size on cruise efficiency and fuel burned is shown in figure 10(d). Cruise efficiency is adversely affected by the somewhat higher compressibility losses for the smaller nacelles. This would result in an increase in fuel burned. However, accounting for the decrease in nacelle friction drag with reduced nacelle diameter, it appears that the nacelle size has almost no effect on fuel burned. Therefore, the optimum nacelle diameter can be selected as that which is conceptually most compatible with the propulsion system design. Nacelle weight was not included in the analysis and decreasing the size would have a favorable effect.

The effects of operating the front and rear propellers at different tip speeds are shown in figure 10(e). Front-to-rear tip speed ratios of 1.1 and 0.9 were analyzed assuming that the average tip speed is 750 feet per second, the same as the baseline which has a 1:1 tip speed ratio. Neither propeller weight nor gearbox weight are appreciably affected and are, therefore, not plotted. The cruise efficiency is slightly lower and the acoustic treatment weight is slightly higher than the baseline CRP for either non-unity tip speed ratio. These changes result in 0.7 percent and 0.4 percent increases in fuel burned at front-to-rear tip speeds of 0.90 and 1.10, respectively.

A third tip speed perturbation was analyzed that consisted of a 10-bladed single rotation prop-fan operating at 750 feet per second tip speed and followed by seven, non-rotating swirl recovery stators (infinite tip speed ratio CRP). This configuration has an efficiency level that surprisingly is only 1.1 percent lower than the baseline CRP. While the SR prop-fan efficiency is appreciably lower, the swirl recovery stators produce additional thrust. Although this is an apparently simpler system with a lower acoustic treatment weight, the lower efficiency, heavier propeller (rotating and non-rotating blade rows) and heavier gearbox increases fuel burned by 1.9 percent relative to the baseline CRP. From the analysis it was also evident that the thrust addition on the stators was very sensitive to small changes in flow incidence. The efficiency of this configuration would deteriorate significantly at off-design conditions. Some of the efficiency loss could be eliminated with variable geometry stators, but at the expense of a heavier and more complex system.

Figure 10(f) shows that reducing the diameter of the rear blades relative to the front blades has very little effect upon performance, noise (acoustic treatment) and fuel burned. This parameter was incorporated in the CRP geometry optimization as it was felt that varying the front and rear diameters might reduce aerodynamic interaction noise and improve efficiency. Although the analysis particularly focused on the tip vortex interference, the calculated effects were found to be negligible at the 0.80 Mach cruise condition. Aerodynamic interference was not found to be a principal noise source for the CRP configurations and it is generally found that performance is even less susceptible to interference sources. The diameters of the front and rear blades were varied such that the average diameter was held constant.

Although the focus was at 0.80 Mach cruise in the parametric study, some consideration was given to other mission conditions. The CRP is required to meet the FAR 36 Stage 3 far-field noise levels, and at the associated low speed conditions aerodynamic interference does contribute to the overall noise. A smaller rear propeller diameter could be effective in reducing this noise source. Low speed performance, however, is adversely affected.

UNUSUAL FEATURES - In additon to the relatively conventional perturbations just discussed, a number of unusual features were also screened. They were conceived as offering tip loss alleviation, source noise reduction, or both. Whereas sophisticated

analytical methodology was used to analyze the previous parameters, the unusual features listed in Table 3 could not be adequately analyzed with available methodologies. Therefore, their effects were investigated on the basis of simplified analyses and judgment.

Only tip devices (proplets) and front blade blowing offered any potential improvement. The effects of proplets were previously estimated in NASA funded studies (4) based upon induced drag reductions that had been demonstrated experimentally for wings with winglets (5). Blade blowing effects were estimated for reducing propeller tip losses. Either of these features is likely to necessitate blade compromises to accommodate them, although no efficiency degradations were estimated for such compromises. For single rotation prop-fans, blade leaning was found to require performance and near-field noise level compromises in order to provide a structurally acceptable design. Counter rotation propellers would be similarly compromised. Counter rotating pusher rather than tractor prop-fans have no effect on cruise efficiency. Because disc spacing is a minor performance consideration, a push/pull configuration--one tractor and one pusher propeller--has a small effect on cruise efficiency.

FINAL CRP CONFIGURATION - Based on the foregoing parametric results, the recommended counter rotation propeller configuration changed somewhat from the original baseline. The number of blades was increased to 12, the total activity factor was lowered slightly, the tip speed raised to 750 ft/sec, the cruise power loading increased to 37 SHP/ft^2, the nacelle diameter decreased to 25 percent of the propeller diameter, and finally, the power split changed to 55 percent front/45 percent rear (fig. 11). The last modification stems from the choice of gearbox type which is addressed later. The overall aerodynamic performance of 89.1 percent cruise efficiency compares favorably with the 80 percent value determined by similar detailed analysis for single rotation propellers.

ACOUSTICS

The noise produced by a CRP differs from that produced by a SRP in two major areas. First, aerodynamic interaction occurs in which the upstream rotor produces wakes which cause interaction at the downstream rotor. Second, acoustic interaction occurs between the two rotors. Due to rotor separation and opposite direction of rotation, the acoustic signals from each combine at field points with differing phase.

The aerodynamic interaction for the original 10-bladed baseline configuration at 700 ft/sec tip speed and 0.8 Mach number cruise is illustrated in figure 12. The upstream rotor, on the left, has a rotational component of 595 ft/sec at the 85 percent radius and a flight component of 778.5 ft/sec. The downstream rotor, on the right, experiences a fluctuating inflow which varies from nearly the resultant of the flight component and its rotational component to the total resultant including the axial and circumferential components of the potential flow of the upstream rotor. This is indicated in the figure by the solid and dashed resultant lines, respectively. Because of the particular orientations of the vectors, the resulting inflow angle change is only 1.1 degrees peak at the downstream rotor. The resulting relative velocity varies from 980 ft/sec to 1076 ft/sec. It is apparent that the potential flow wake interaction effects are small. A second blade wake component is that due to viscous drag. The viscous wake is also indicated in figure 12. This wake component results in a velocity deficit due to the drag of the blade airfoil section. This component generally results in a greater air angle change. In this example, the viscous wake has the potential for a 5-degree change in the downstream rotor angle-of-attack. Although the axial components of the potential and viscous wakes almost cancel each other, their circumferential components add. The total wakes show a peak downstream rotor angle-of-attack change of about 5.5 degrees.

Each upstream rotor blade produces a wake which is intercepted by the downstream rotor. Figure 13 shows a typical wake as experienced by the downstream rotor. The wake has been resolved into axial and tangential components. In the axial direction, the potential flow and viscous wake components have opposite direction and tend to cancel. In the tangential direction, the two components add. It should be noted that the wakes are relatively narrow, typically indicating high frequency components. Although the peak tangential component is significant, at about 15 percent of free stream velocity, the narrowness of the wake indicates that there is not really much energy in the wakes.

The effect on noise of unsteady loading on the downstream rotor due to interaction with the wakes from the upstream rotor is summarized in figure 14. This figure is a polar plot of the noise levels for the first three harmonics of loading noise produced by the downstream rotor. The interaction pattern has 10 lobes which is a result of 5 blades interacting with 5 wakes. Since the

upstream and downstream rotors turn in opposite direction, each blade of the downstream rotor intersects the upstream blade wake twice in each revolution. This produces 10 wake intersections for each downstream rotor revolution, hence the 10-lobed pattern. A second item of note is that the unsteady loading effects are small. At the fundamental of the blade passing frequency (BPF) the effect is only about ± 1 dB. A cycle extending over 36 degrees may be seen. This occurs because the steady and unsteady components are in phase for half this cycle and out-of-phase for the other half. A larger effect occurs for the second harmonic because the harmonic number (2) times the blade count (5) equals 10, which couples better with the 10-wake pattern. At the third harmonic, the wake-interaction effects are again small. It is thus apparent from figure 14 that the aerodynamic interaction effects are small. The resulting unsteady loading noise is not a very significant component.

From an acoustic standpoint, the two rotors can be considered as two sources of noise. Since they are rotating in opposite directions, their acoustic signals at a given field point will have different arrival times. If the two rotors rotate at the same speed, as is normally the case, the difference in arrival times of the acoustic signals from the two rotors is variable depending on the location in space. Thus, there will be acoustic interaction between the two rotors. In fact, there will be field points where the acoustic signals arrive in phase. At these points, the noise produced by the CRP is like that of a single 5-bladed rotor, but having levels which are 6 dB higher. There are also field points where the acoustic signals arrive exactly out of phase. At these points, the acoustic signature looks like that of a single rotor having the same total number of blades (10 in this case) since the odd harmonics cancel.

It should be noted that cancellation occurs only when the acoustic signals from the two rotors are identical. In general, this is not the case, as the downstream rotor has a different signature due primarily to the aerodynamic interaction. However, as previously shown, the aerodynamic interaction during cruise is small so the acoustic signatures from the two rotors are very much the same.

Figure 15 shows a summary of the near-field noise components of the CRP in cruise compared to the noise of an equivalent SRP. (In this context, "equivalent" means the same diameter, same tip speed, same total power, and same total number of blades.) The loading noise component, which is the only one influenced by aerodynamic interaction, is seen to be small beyond the first harmonic. The remainder of the spectrum is mainly thickness noise and quadrupole noise. The upper short horizontal bars indicate the peak levels which occur when the acoustic signals combine in phase. It should be noted that the spatial positions for which this occurs are not necessarily the same at each harmonic. Also shown, are the minimum values, which occur when the acoustic signals are out of phase. At the 1, 3, and 5th harmonic, the acoustic signals almost cancel perfectly. This is the case for which the acoustic signal of the CRP is essentially like that of the equivalent SRP. Advantage of this azimuthal directivity could be taken by placing the fuselage in one of the "valleys." However, since a 5 by 5 bladed CRP produces the 10 lobes, the valleys are only 36 degrees apart. This angle is small compared to the included angle defined by a typical fuselage so that several peaks and valleys would occur on the surface. The space averaged total noise on an energy basis is shown by the solid line. The SRP has energy only at even harmonics of a 10-blade propeller as shown by the large circles. Compared to the noise of a SRP, the total acoustic energy of the CRP is about the same, mostly because the aerodynamic interaction is small. However, in a spatial average, the CRP has all the frequency components of a single rotor.

Figure 16 shows the impact of the additional frequency components of the CRP on cabin noise. For this example, the cabin noise of a CRP-powered airplane is compared with that of a SRP-powered airplane having identical fuselage acoustic treatment. It was assumed that the signal attenuation through the fuselage sidewall obeyed the mass-law relation--attenuation proportional to the mass times the frequency. The source noise levels are the space-averaged levels of the CRP and those of an equivalent SRP. The spreading of the acoustic energy over a broader frequency range results in the cabin noise for the CRP being 1.6 dBA higher than that for the SRP. This occurs mostly due to the low frequency component, as the fuselage acoustic treatment is less effective at lower frequencies.

Synchrophasing can also be used to further offset interior noise or treatment weight penalties. However, the benefit would be comparable for SRP and CRP.

Both the aerodynamic and acoustic CRP configuration optimization were done for the 0.8 Mach number cruise condition. However, it is also required that an airplane powered by CRP be certifiable from a noise standpoint. Thus, there is an acoustic

constraint for takeoff and approach conditions; namely, that the airplane meet FAR Part 36, Stage 3 noise requirements.

From the aerodynamic trade study on tip speed and power loading, it may be recalled that the curve of fuel burn versus tip speed minimized at a tip speed of 750 ft/sec and a SHP/D^2 of 36.8. At these conditions, it is apparent from Table 4 that the far field noise limits can be met, assuming moderate additions for engine and airframe noise contributions.

VIBRATORY AERODYNAMIC EXCITATIONS

Two factors which determine the stressing of the propeller blades are the vibratory aerodynamic excitations and the propeller dynamic response characteristics. The structural design of the blades are strongly influenced by these factors.

AERODYNAMIC EXCITATION - The primary vibratory aerodynamic excitations are caused by the angular and distorted flow field in which propellers operate. The major aerodynamic excitation occurs at frequencies of one times the rotational speed, 1P, because of the angular inflow into the propeller caused by the wing circulation, inclined airflow aircraft geometry and aircraft wake effects. This 1P excitation depends on the wing loading and can be controlled to some extent by nacelle length and tilt.

The worst 1P aerodynamic excitation usually occurs for maximum aircraft gross weight at the minimum climb speed without deployed flaps, and would be the same for the CRP and SRP except for the flow straightening effects of the front and rear rotors on each other due to induction effect. An approximate analysis of a typical swept wing prop-fan aircraft with 11.4 feet diameter, 12-bladed, 12,000 HP prop-fans indicates that the angularity of the flow into the front rotor would be decreased about 8 percent by the induction effects of the rear rotor and that the rear rotor angularity would be decreased about 18 percent. However, it is believed that other effects such as the increase in flow velocity and the straightening effect on SRP from induction would decrease this angular improvement in 1P excitation to about 5 percent and 10 percent respectively. Experimental tests are required to determine the actual 1P excitation improvement of CRP's over SRP's.

The only significant higher order flow field excitation is usually due to wing sweep that occurs at a frequency of 2P. It is doubtful that the induced effects of the rotors on each other will significantly affect the magnitude of the 2P excitation or any other even order excitation because of flow symmetry. While the higher order CRP excitations are predicted to be of the same order as those for the SRP, the dominant excitation is 1P where the CRP configuration is superior (fig. 17).

The CRP will also have excitations due to blade passage wakes at a frequency of NP, where N is the total number of blades. A cursory analysis using the resulting loadings from the acoustic analysis shows that the blade passage loadings are very low. This result is supported by information in the literature, Hamilton-Standard experience in the 1940's, and the experience with the Shackelton bomber.

DYNAMIC CHARACTERISTICS - The effect of the aerodynamic loads can be magnified by the dynamic characteristics of the propeller. Propellers react dynamically with an aircraft in one of the three modes (reactionless, whirl, or symmetric) as illustrated in figure 18. Without sychrophasing, the CRP will react with the aircraft with twice as many whirl and symmetrical modes as an equivalent SRP because it is the number of blades per rotor and flow field excitations that determine these modes; e.g., for a 6 x 6 bladed CRP whirl modes will occur at 5P and 11P (forward) and 7P and 13P (backward), whereas for an equivalent 12 bladed SRP only the 11P (forward) and 13P (backward) whirl modes occur. Likewise the 6 x 6 bladed CRP symmetrical modes will occur at 6P and 12P whereas they occur only at 12P for the 12 bladed SRP. However, with phasing (between disks) and synchrophasing (between engines) it is possible to make the CRP symmetrical modes (6P and 12P) cancel. Without synchrophasing and proper phasing, the symmetrical modes can combine so that they beat or add in which case they can be as great as the 12P excitation of the SRP. In addition, the 6P excitation is a symmetrical mode for the CRP whereas it is reactionless for the SRP.

By proper phasing and synchrophasing it is also possible to make the propeller loads on the aircraft due to the whirl modes combine to form linear loads, thus resulting in smoother aircraft operation. However, the 5P and 7P loads of the CRP will still react with the aircraft at 6P, whereas these corresponding excitation modes are reactionless for the SRP. Thus without proper phasing and synchrophasing, the CRP aircraft will be subjected to more reaction modes than a SRP aircraft (6 vs.3). With proper phasing and synchrophasing this ratio can be reduced to 4 vs. 3.

Because the required phasing of the two rotors will differ for the whirl and symmetrical modes, the optimum phasing will be a compromise to be determined by test and/or sophisticated analysis. This is similar to synchrophasing on multi-propeller SRP aircraft except that cancelling or minimizing excitation loads at the single CRP source is more beneficial for overall aircraft smoothness. The significance of these results is that the CRP aircraft will experience slightly higher prop-fan aerodynamic excitation loadings; however, the impact should be small with proper phasing and synchrophasing.

Similarly the propeller blade response characteristics should be about the same for CR and SP propellers except for blade retention and aircraft impedance effects.

A review of likely blade natural frequencies shows that the blade critical speeds for the lower blade modes will be well below the operating speeds, and, therefore, there will be little magnification of the blade passage excitations.

A cursory evaluation was also made of (1) CRP whirl flutter stability and its effect on aircraft stability and (2) stall and classical flutter stability as they affect the propeller. Counter rotation helps the whirl flutter stability by eliminating the gyroscopic coupling and cross aerodynamic moments increase stiffness. Because stall flutter is usually an individual blade phenomenon and a function of blade loading and torsional natural frequency, stall flutter for the CRP should be about the same as for the SRP. Similarly it is felt that classical flutter stability for the CRP will be the same or slightly better than for a SRP of the same number of blades. This is due to the lower aerodynamic coupling between the blades.

The brief vibration evaluation indicated that there are no apparent adverse effects due to counter rotation. In fact, there are a number of areas in which the CRP should be better than the SRP. Some of these benefits pertain to the propeller itself, but a number have a significant effect on the aircraft from control and structural standpoints. The aircraft related benefits include lower 1P aircraft steady loads, better whirl flutter stability, and elimination of gyroscopic loads.

COUNTER ROTATION GEARBOXES

Since counter rotation propellers presumably require complex gearboxes an effort was initiated to assess this issue. The general approach was to consider a wide variety of potential gearbox configurations, perform a screening process to narrow the field of candidates to only a few, and then evaluate these chosen few in enough depth to adequately characterize advanced technology CR gearboxes.

This process began with a literature survey that identified counter rotating reduction gear systems built from the late 1940's through the 1970's. The survey identified approximately twenty counter rotating gearbox applications covering turbine engines, reciprocating engines, and helicopter rotors. Significant design and operating characteristics such as power, speeds, torque, number of stages, weight, size, and efficiency were compiled. Information on gearbox life, maintenance cost, replacement cost, and noise was not available in the open literature.

Of all the concepts surveyed, only two have a significant amount of operating time: (1) the differential planetary used in the Russian NK12M turboprop engine (for the TU95, TU114, and AN-22 aircraft) was introduced to service in 1958 and is still used today, and (2) the spur with reversing idler reduction gear system for the Rolls-Royce Griffon reciprocating engine in the Shackelton aircraft has been in service since 1950. As a result of the survey, five in-line and five offset reduction gear concepts which merit further investigation were identified.

IN-LINE CONCEPTS - The five in-line concepts, illustrated in figure 19, include the differential planetary, split path planetary, compound planetary, planetary with reversing bevel, and multiple compound idler concepts.

The differential planetary concept is the simplest epicyclic (planetary) system for counter rotation. The front prop is driven through the planet pinion carrier while the rear prop is driven through the ring gear. The front prop rotates in the same direction as the input shaft while the rear prop rotates in the opposite direction. The equilibrium torque distribution for each prop is fixed by the geometric design considerations related to gear diameter. The propeller power split corresponds to the torque split when the prop speeds are equal and opposite. The power split and relative propeller speed is controlled by the blade pitch of each propeller.

The split path planetary concept converts the differential planetary configuration to a grounded system with a fixed speed ratio to each propeller. As in the differential planetary, the planet pinion carrier drives the front prop while the ring gear

drives the rear prop. Front prop and input shaft rotate in one direction while the rear prop rotates in the other direction. Multiple bevel idler gears are supported by the gearbox housing grounding the differential planetary system and imposing equal and opposite propeller speeds at any propeller power split. Changes in propeller pitch in this system cannot influence the propeller power or speed split which could simplify the propeller pitch control for this system relative to the differential planetary system. The bevel idler gears carry about 10 percent of the rear prop power when the power split between the propellers is equal.

The compound planetary concept is an alternate approach to a grounded planetary system. As in the differential planetary concept, the planet pinion carrier drives the front prop while the ring gear drives the rear prop. The planet pinions are dual diameter (tandem) pinions with the smaller pinion engaging the grounded ring gear. The diameter of the grounded ring gear establishes the speed of the planet pinion carrier and the front propeller. The diameter of the grounded ring gear can be selected to impose equal and opposite propeller speeds regardless of propeller power split. This concept with the rear propeller shaft removed is representative of a single rotation propeller system used extensively (Rolls Royce Tyne turboprop engine).

The planetary with reversing bevel configuration represents an "add on" conversion of a single rotation propeller drive to achieve counter rotation. This system was used in the reciprocating Pratt & Whitney R4360 engine. The front propeller is driven through the planet pinion carrier while the ring gear is grounded to the gearbox housing as arranged in the single rotation planetary system. Counter rotation is provided by driving the rear propeller through a multiple bevel idler gear from the front propeller shaft. One hundred percent of the rear prop power is carried by the bevel idler gears at any power split between the propellers.

The multiple compound idler or multiple layshaft concept, provides counter rotation with an in-line input shaft using fixed parallel shafts. Three or more intermediate speed idler shafts are evenly spaced around the gearbox centerline. Power is distributed evenly to the idler shafts with a self-centering input pinion or equivalent load sharing device. The front propeller is driven through the idler shafts with a single output gear having external teeth while the rear propeller is driven with the larger output gear having internal teeth. The speed of each propeller is fixed by the geometric gear diameters and is not affected by power split.

OFFSET CONCEPTS - The offset counter rotating gearbox configuration candidates include dual compound idler, spur with reversing idler, dual compound idler with reversing idler, compound bevel, and spur differential planetary concepts (fig. 20).

The dual compound idler concept is an offset shaft version of the multiple compound idler parallel shaft system discussed above. This concept is based on previous studies which found this system to be an attractive single rotation reduction gear concept. Two intermediate speed idler shafts are located between the input and propeller shafts, one on each side of the gearbox mid-plane established by these shafts. This arrangement functions identically to the in-line version.

The spur with reversing idler concept is the simplest fixed parallel shaft system for counter rotation. This concept has been used extensively with reciprocating engines including the Rolls Royce Griffin and Merlin engines. The front propeller is driven directly by an output gear which meshes with the input pinion gear. The rear propeller is driven through an idler gear which meshes with a second input pinion and a corresponding output gear. The rear propeller pinion and gear diameters are smaller than the front propeller diameters to avoid direct engagement, allowing the idler to reverse the rear propeller rotation relative to the front propeller.

The dual compound idler with reversing idler concept replaces the internal output gear of the dual compound idler concept with an external output gear and reverser idler. The power distribution between the idler shafts and between the propellers follows the principles of a dual compound idler concept. The propeller speeds are fixed by geometric gear diameter relationships.

The compound bevel concept is the simplest fixed non-parallel shaft system for counter rotation. This system has been used in helicopter applications by Gyrodyne. A single intermediate speed idler shaft is located at right angles to propeller shafts. The idler shaft is driven by a bevel gear which engages the input bevel pinion located at any convenient angle. The front propeller is driven by an output bevel gear which engages the aft side of the idler pinion while the rear propeller output bevel gear engages the front side of the idler pinion.

The spur differential planetary concept converts the in-line differential planetary system to an offset shaft arrangement which improves access to the propeller pitch control components in the output shaft. The planetary sun gear is driven through a quill shaft from a spur gear engaging an input shaft pinion. The sun gear speed may be designed to be equal to or less than the input speed from the turboshaft engine. As in the in-line differential planetary system, torque distribution to each propeller is fixed by the gear diameter ratio and the relative propeller speed is controlled by the blade-pitch angle of each propeller.

GEARBOX CONCEPT SCREENING - The in-line planetary with reversing bevel and the offset spur with reversing idler reduction gear concepts were eliminated from further consideration because a gear ratio of approximately 10, consistent with turbine engine designs, could not be met with these systems. Both of these systems were utilized in reciprocating engines where the gear ratio was in the 2 to 3 range. The remaining eight concepts were subjected to a "forced decision" screening process (6) that involved experienced personnel establishing a set of weighting factors for each of the evaluation parameters: reliability, efficiency, maintenance, acquisition cost, weight, technical risk, ease of sealing, acoustical signature, spatial envelope, and pitch control accessibility (a factor in maintenance but considered important enough to be identified separately). The assessments were based on an analysis of each gearbox concept that included sizing the gears and bearings, and sketching each configuration to identify the number of bearings, gears, and the output shaft and propeller pitch control spatial envelope requirements. To size the gears, the gear diametral pitch, pitch diameter, gear face width, bending stress, contact stress, rim thickness, and tooth rib and web volume were determined. To size the bearings, the mean load capacity B10 life, and envelope dimensions and volume were determined. From this information, preliminary estimates of efficiency, acquisition cost, weight, maintenance requirements, pitch control accessibility, and spatial envelope were made. Judgement of experienced personnal was used to assess the reliability, technical risk, ease of scaling and acoustical signature. Both the weighting factors and the design evaluation assessments were reviewed with staff members of Pratt & Whitney, Hamilton-Standard, and Sikorsky Aircraft.

The "forced decision" analysis led to a figure of merit that was used to select the best in-line and the best offset reduction gear concepts. The figure of merit is the sum of the products of the weighting factors and design evaluation assessment raw scores determined for each of the ten parameters. The assessment raw scores could range from 0 (minimum) to 1 (maximum).

Tables 5 and 6 display the details of this process, and the total weighted score for each concept. These scores are compared in figure 21. The differential planetary concept scored significantly higher than any other in-line configuration. Among the offset reduction gear concepts, the dual compound idler and spur differential planetary systems are approximately equal in value. Therefore, the concepts selected for further evaluation included (1) differential planetary in-line, (2) dual compound idler offset, and (3) spur differential planetary offset.

Figure 22 summarizes the results of this evaluation including sketches that are approximately to scale. The in-line differential planetary configuration has the fewest number of gears and bearings and highest reliability. However, it does have a disadvantage in that the propeller pitch control accessibility is the worst of the three systems evaluated. In fact, it likely will require complete removal of the gearbox from the aircraft. The impact of this is to reduce the mean time between removals (MTBR). Nevertheless, since the differential planetary configuration is the most efficient, the lightest, and the least expensive of the candidates, it still yields the lowest mission fuel and the lowest airplane DOC.

GEARBOX TECHNOLOGY - The technology level used in the gearbox study is consistent with that being currently investigated in various government and industrial programs for the 1990 time period assumming adequate funding. It represents a substantial improvement over current technology as detailed in Table 7. The advanced transmission technology materials and sophisticated design techniques would markedly increase system reliability while reducing weight. An indication of weight improvement over early technology is given in figure 23. Noted on this figure is information available from the open literature on a number of existing or early counter rotation reduction gear systems including the Double Mamba, Python, Allison T40 and the Russian NK-12 engine gearbox. The estimated weight decrease for an advanced 12,000 SHP CR gearbox is 15 to 20 percent.

AIRPLANE/MISSION BENEFITS

To determine the impact of counter rotation advantages in a typical commercial

transport application, a representative 100-passenger, Mach 0.8 cruise speed, twin-engine airplane was defined by Lockheed-Georgia. A low-wing configuration was selected with 1300 nautical mile range capability at full load. Other design parameters were compatible with the CR propeller/gearbox tradeoff analysis (i.e., 82 dBA cabin noise limit, FAR 36-Stage 3 exterior noise constraint, approximately 12,000 take-off SHP per engine, and a baseline propeller-fuselage clearance ratio of 0.8 (clearance/propeller diameter)).

This airplane was sized using the advanced CR propeller and gearbox configurations determined from the tradeoff analyses and compared with an advanced 10-bladed SR prop-fan powered version. Both the SR and CR powerplant definitions used in this comparison are displayed in figure 24. While the in-line differential planetary gearbox was selected for the CR system, the offset compound idler configuration was selected for the SR gearbox based on a separate study (7). The difference in gearbox types selected reflects differing requirements between SR and CR. For example, SR in-line planetary gearing involves such high centrifugal loads in the planetary pinion bearings that very short bearing life results--a problem absent in CR planetary systems since the centrifugal loads are reduced due to the carrier not being grounded. In general, in-line concepts are more suitable for CR than they are for SR. On the other hand, a drawback of in-line systems for either SR or CR is the somewhat higher maintenance cost caused by propeller pitch control inaccessibility. If this drawback could be substantially mitigated the in-line system would be competitive for SR also. In any case, the choice of gearbox types is not too important when comparing SR and CR benefits since the best SR in-line concept (split-path) is only slightly worse than the best SR offset concept (compound idler) on a DOC basis (7).

The potential benefit of using an advanced technology counter rotation system is illustrated in figure 25 for 400 nautical mile trip. A fuel saving of 8 percent and a DOC reduction of 2.5 percent is estimated. Based on previous analyses, these savings would not be materially altered at different trip lengths, cruise altitudes, or payload. An advanced counter rotation propeller system (CRP) is projected to have an 8 percentage point higher efficiency due to swirl recovery and a higher blade count, with only a 12 percent increase in propeller weight and 1.6 dBA cruise interior noise increase. With a compact differential planetary gearbox (similiar to the approach used on the Russian Bear Bomber), the required 9.7 to 1 gear ratio can be obtained in only one stage. This results in a 15 percent lighter gearbox with a 0.2 percent higher efficiency than the system required for single rotation turboprops. There does appear to be an increase in acquisition and maintenance cost with the in-line CRP gearbox. However, because of the small size and light weight of this gearbox, it may also be possible to locate it between the two rotors (interprop) for additional system benefits. Integration of the CRP propulsion system with the aircraft offers some additional advantages. These include cancellation of torque and gyroscopic loads, enhanced aircraft flutter stability and improved aerodynamic integration due to slipstream swirl removal. However, with the slightly higher CRP propeller interior noise (1.6 dBA) and lower frequency noise content, the cabin acoustic treatment weight may have to be increased by about 5 percent (0.14 percent of aircraft gross weight). Based on these performance and weight changes, an 8 percent block fuel savings and a 2.5 percent DOC reduction is estimated for an advanced CR system relative to a comparable SR system.

CONCLUSIONS

The CRP fuel savings and DOC benefits are large enough to warrent continued activities. No serious problems were identified that might preclude realizing these benefits through a sound R&T program. Of course, even though the CR concept was subjected to modern sophisticated aerodynamic performance and acoustic analyses, this is clearly an area where experimental confirmation of the predicted attributes is required before unequivocal endorsement of CR is appropriate.

Meanwhile, continued analytical investigation would be worthwhile to (1) establish better acoustic and vibration predictive techniques and (2) extend the current analyses to other applications, potential solutions to the in-line gearbox pitch change accessibility issue, and more off-design investigations. The basic technology for advanced CR prop-fans and gearboxes is identical to that for SR propellers and gearboxes, at least as far as current understanding permits. But the challenge of verifying that advanced design techniques can be utilized to lessen the complexity and maintenance drawbacks remains. Counter rotation is an area that deserves continued attention in our pursuit of advanced propulsion systems.

ACKNOWLEDGEMENTS

The authors wish to thank the following people who helped in the preparation of this paper.

Hamilton-Standard
D. Black
B. Magliozzi
R. Cornell

Pratt & Whitney
A. McKibbin
G. Pagluica

Lockheed Georgia
D. Byrne
N. Searle
M. Walsh

REFERENCES

1. Standard Method of Propeller Performance Estimation. Society of British Aircraft Constructors, Ltd.

2. D. Biermann, and W. H. Gray "Wind-Tunnel Tests of Eight Blade Single and Dual-Rotating Propellers in the Tractor Position," NACA Wartime Report L384, 1941. National Aeronautics and Space Administration, Washington, DC.

3. Weight Prediction Mannual, The Boeing Company D6-23201TN.

4. D. M. Black, B. Magliozzi, and C. Rohrbach "Small Transport Aircraft Technology Propeller Study" (to be published).

5. J. J. Spillamn "The Use of Wing Tip Sails to Reduce Vortex Drag," Aeronautics Journal, Vol. 82, Sept. 1978, pp 387-395.

6. J. Fasal "Forced Decision for Value." Walter Kiddie Co. Product Engineering, April 1965.

7. J. Godston and J. Kisn "Selecting the Best Reduction Gear Concept for Prop-Fan Propulsion Systems," AIAA 82-1124, Joint Propulsion Conference, Cleveland, OH, June 1982.

APPENDIX - WEIGHT EQUATIONS

This appendix defines the generalized weight relationships used in the determination of the "optimized" propeller discussed in the text for a Mach 0.8, low-wing, twin-engine, 100-passenger airplane. Units are pounds, feet, second, and degrees.

Propeller, W_{prop}

$$W_{prop} = 3.37 \times 10^{-4} \times (\text{Diameter})^{1.846} \times (\text{No. of blades})^{-0.05} \times (\text{Total activity factor})^{0.75} \times (\text{Takeoff tip speed})^{0.3} \times (\text{Takeoff shaft horsepower})^{0.327} \times [1 + 0.1\ (\text{sweep angle}/40)]$$

Gearbox, W_{GB}

$$W_{GB} = 942. \times (\text{Gear ratio}/8.63)^{0.15} \times (0.8125 \times \text{Torque Factor} + 0.1875) + \text{Spacing Weight}$$

Where, Torque factor = actual torque/baseline torque

Spacing weight =

133. (DS - 1.75) for propeller disk spacing (DS) $\leq$ 2.5 ft.

550. (DS - 2.5) + 100 for DS > 2.5 ft.

Acoustic Treatment, W_{AT}

$$W_{AT} = 0.955 \times (\text{No. of propellers}) \times (\text{Propeller diameter}) \times (\text{Nacelle diameter}) \times \sigma_{REF} \times 212/BPF \times 10^{(dB - dB^*)/20}$$

Where,

	C/D		
	0.672	0.800	0.907
σ_{REF}	5.44	5.60	5.60
dB*	136.2	134.9	134.4

C = clearance between propeller and fuselage
D = propeller diamter

σ_{REF} = Acoustic treatment weight parameter, lb/ft^2
BPF = blade passage frequency, hz
dB* = ref. noise level

Landing Gear, W_{LG}

$$W_{LG} = 2150 + 240\ (D - D_{ref.})$$

Where, $D_{ref.}$ = propeller diameter at 32 SHP/ft^2

Table I. - Historical Counter Rotation Propeller (CRP) Efficiency Gains Over Single Rotation Propellers (SRP)

[Simulated condition: Mach 0.8 cruise at 35 000 ft.]

Shp/D^2	Tip speed	Δ Efficiency points	
		Experimental*	Ideal**
20	600 ft/sec	11	8.6
30	700 ft/sec	11	8.7
40	800 ft/sec	11	8.4

* NACA L-384 8-blade SRP and 4x4 CRP data (isolated).
**SBAC 8-blade SRP and 4x4 CRP

Table II. - Baseline Propeller Definition

[Mach 0.8 Cruise at 35 000 ft.]

Number of blades	10 (5x5)
Blade activity factor	180
Camber (C_{LI})	0.31
Power split (front/rear)	50/50
Tip Sweep "	40° x 40°
Tip Speed Ratio "	1:1
Diameter Ratio "	1:1
Disk Spacing/Diameter	.18
Nacelle/Prop Diameter	.35
Tip speed, ft/sec	700
Power loading, Shp/D^2	32

Table III. - Unusual CR Propeller Features

Feature	Impacts		
	Cruise efficiency	Noise**	
		Cabin	Far field
Tip devices	+1.5%*	0 - 3 dB increase	0 - 1 dB increase
Leaned blades	Negligible	Negligible	Negligible
Unequal number of blades front and rear	Negligible but adverse	0 - 2 dB increase in annoyance	0 - 2 dB increase
Front blade blowing	+1% to +2%*	0 - 1 dB decrease	2 - 3 dB decrease
Differential blade diameters, within a disc	Negligible but adverse	Negligible	Negligible
Pusher or Push/Pull	Negligible	0 - 3 dB increase	2 - 4 dB increase

* Not including blade compromises to accommodate these features.
**Same tip speed and Shp/D^2.

Table IV. - Far-Field Noise Evaluation For CR Propeller

[Propeller noise only; tip speed, 750 ft/sec; SHP/D^2, 36.8.]

Parameter	Flyover		Sideline
	Normal take-off	Cutback	
Diameter, ft	12.33	12.33	12.33
Tip speed, ft/sec	750	700	750
SHP/D^2	78.9	51.3	78.9
Slant distance, ft	3200	2350	1679*
Flight speed, kn	170	170	150

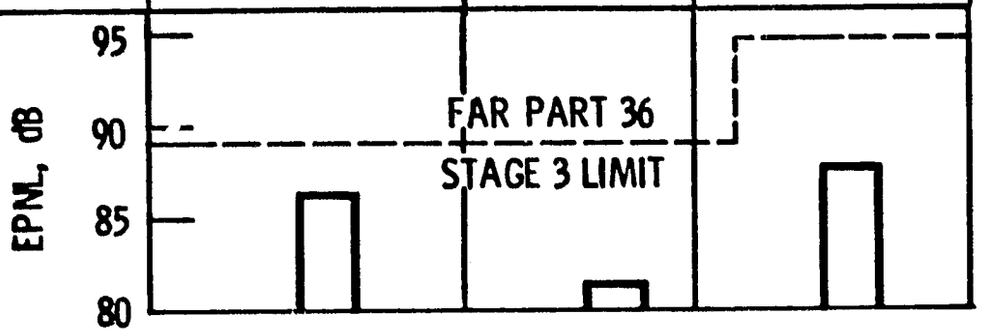

*1476 ft SIDELINE AT 800 ft ALTITUDE

Table V. - In-line Counter Rotation Gearbox Screening

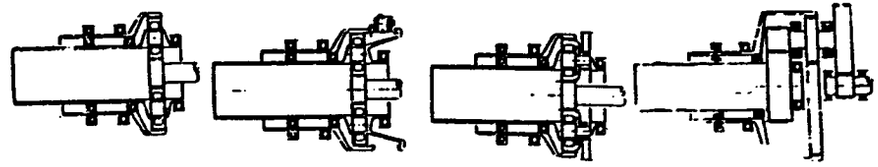

	Weighting factor	Raw score	Weighted score	Raw score	Weighted score	Raw score	Weighted score	Raw score	Weighted score
Reliability	0.18	1.0	0.18	0.86	0.15	0.21	0.039	0.29	0.051
Efficiency	.17	.93	.16	.43	.073	.57	.097	.93	.158
Maintenance	.13	1.0	.13	.86	.112	.29	.037	.14	.018
Acquisition cost	.12	1.0	.12	.57	.068	.57	.069	.29	.034
Pitch control access	.12	.29	.034	.29	.035	.29	.034	0	0
Weight	.11	1.0	.11	.64	.07	.64	.071	.43	.047
Technical risk	.08	.57	.046	.86	.69	.71	.057	1.0	.08
Ease of scaling	.04	.71	.029	.71	.028	.71	.029	.71	.029
Acoustic signature	.03	.71	.021	.71	.021	.21	.006	.71	.021
Spatial envelop	.02	.71	.014	.71	.014	.71	.014	.43	.009
Total Weighted score			0.844		0.640		0.453		0.447

Table VI.- Offset Counter Rotation Gearbox Screening

	Dual compound		Dual compound idler with rev. idler		Compound bevel		Spur differential planetary	
	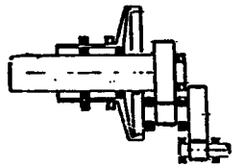				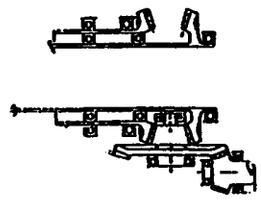		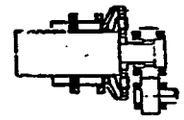	
	Weighting factor	Raw score	Weighted score	Raw score	Weighted score	Raw score	Weighted score	Raw score	Weighted score
Reliability	0.18	0.71	0.129	0	0	0.43	0.77	0.50	0.09
Efficiency	.17	.71	.121	.29	.049	.14	.043	0	0
Maintenance	.13	.71	.092	0	0	.57	.074	.43	.056
Aquisition cost	.12	0	0	.14	.017	.57	.069	.86	.103
Pitch control access	.12	.79	.094	.79	.094	.79	.094	.79	.094
Weight	.11	.21	.024	.21	.024	0	0	.86	.094
Technical risk	.08	.29	.023	0	0	.14	.011	.43	.034
Ease of scaling	.04	.14	.006	.14	.006	.14	.005	.71	.029
Acoustic signature	.03	.71	.021	.43	.013	1.0	.03	0	0
Spatial envelope	.02	.29	.006	.07	.001	.071	.001	1.0	.02
Total weighted score			0.516		0.204		0.385		0.52

Table. VII. - Gearbox Technology Comparison

	Current technology	Technology assumed available by 1990
Gears		
Materials	AMS 6265	Vasco X-2M or Cartech EX-53
Bending fatigue limit		
Unidirectional, psi	50,000(1)	60,000(1)
Reversed bending, psi	41,000(1)	49,000(1)
Hertz stress, psi	126,000(1)	151,000(1)
Pitch line velocity, ft/min	30,000	35,000
Bearings - M50 CVM material		
System design life (B10), hr	18,000	18,000
Material/lubrication life factor	6 to 12	20 to 30
Housings	Al;	Advanced, aluminum, magnesium, and/or stainless steel
Lubricant	MIL 23699 type II	Synthesized hydrocarbon fluid
Allowable temperature rise, °F	40 - 50	80 - 100
Load carrying ability, lb/in	2000 - 3500	4000 - 4500
Flash temperature index, °F	276	350

(1) Typical gear allowable stress - 3 sigma with a coefficient of variation = 0.1, 10^{10} cycles

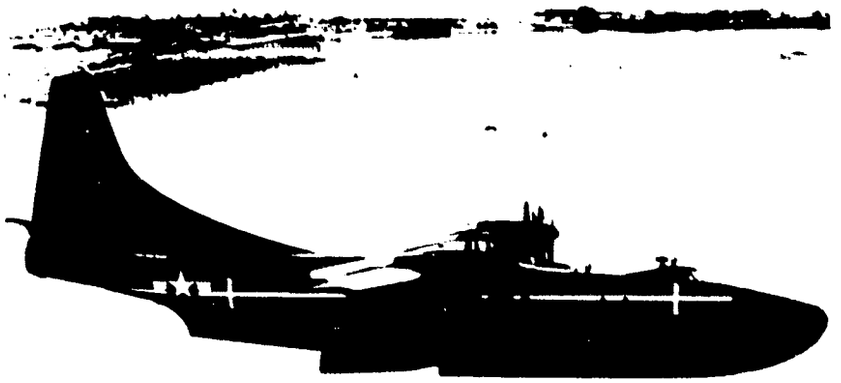

Figure 1. Counter-rotation airplanes.

ORIGINAL PAGE
BLACK AND WHITE PHOTOGRAPH

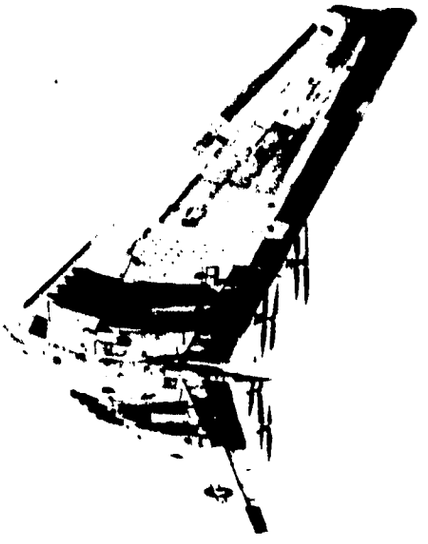

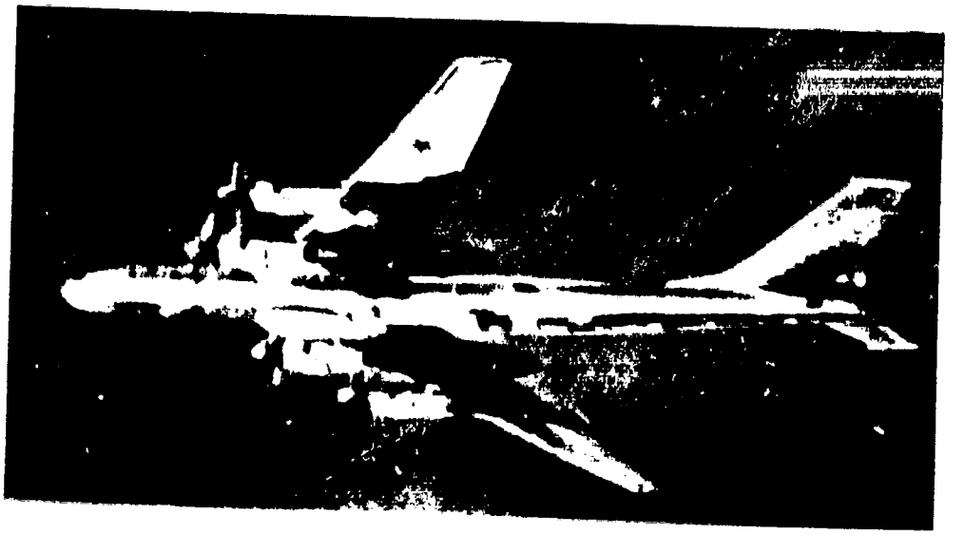

Figure 1. - Concluded.

Figure 2 - Russian tupolev TU114 transport aircraft with CRP.

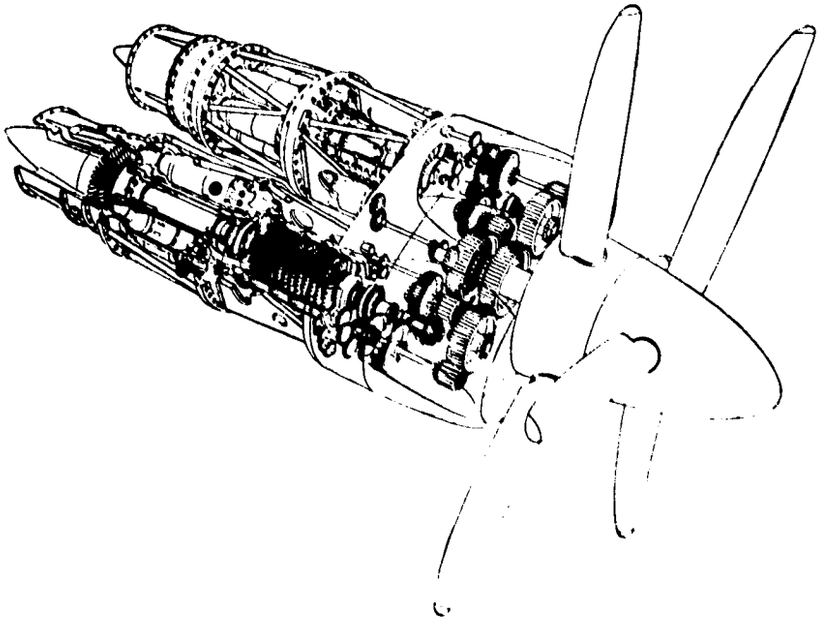

Figure 3. - Coupled naiad (1960).

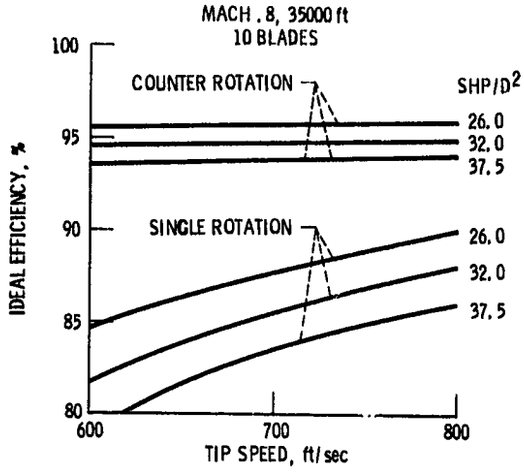

Figure 4. - Historical data.

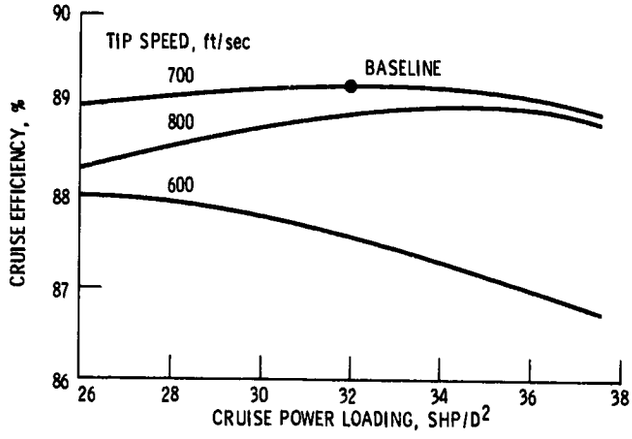

Figure 5. - Tip speed and power loading optimization.

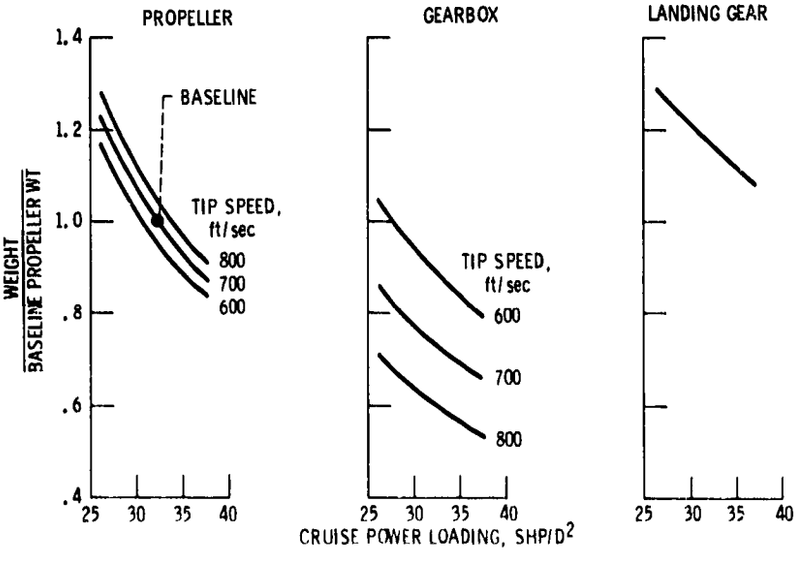

Figure 6. - Weight summaries for aerodynamic optimization.

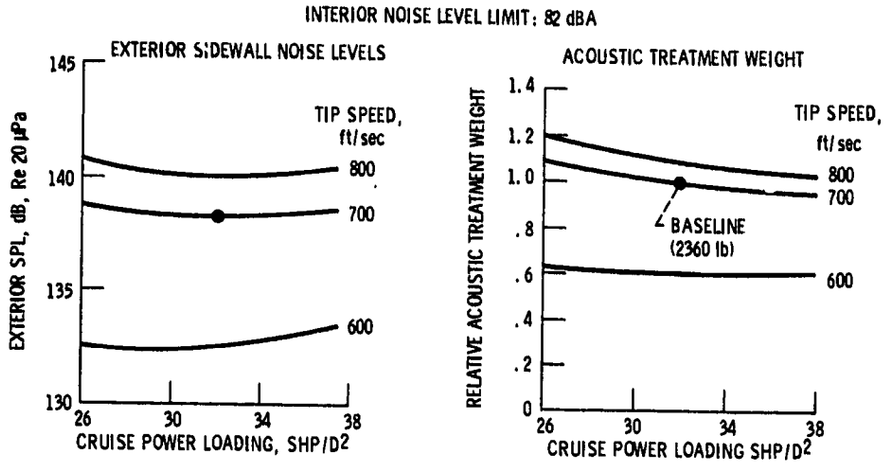

Figure 7. - Cabin acoustics for aerodynamic optimization.

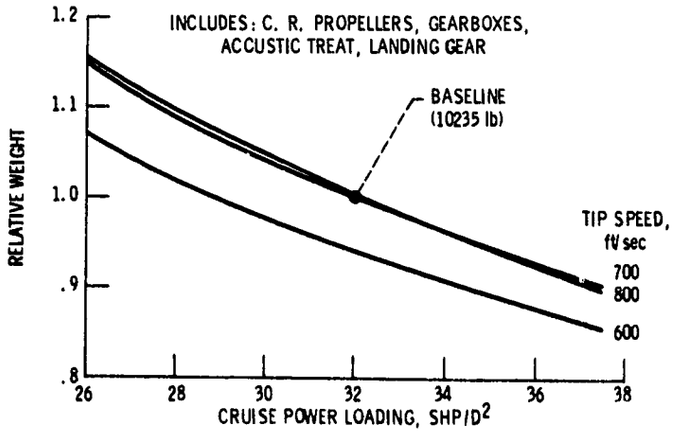

Figure 8. - System weight summary.

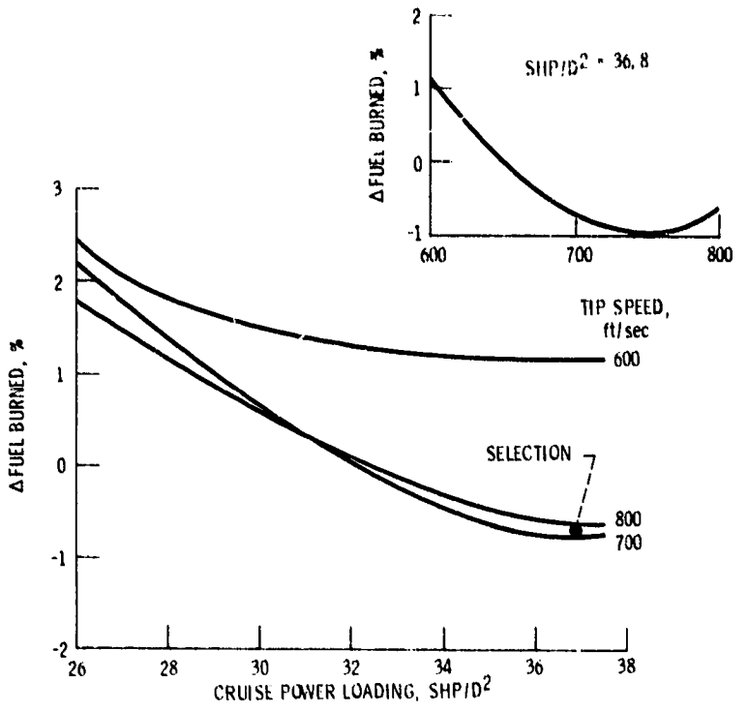

Figure 9. - Fuel burned summary.

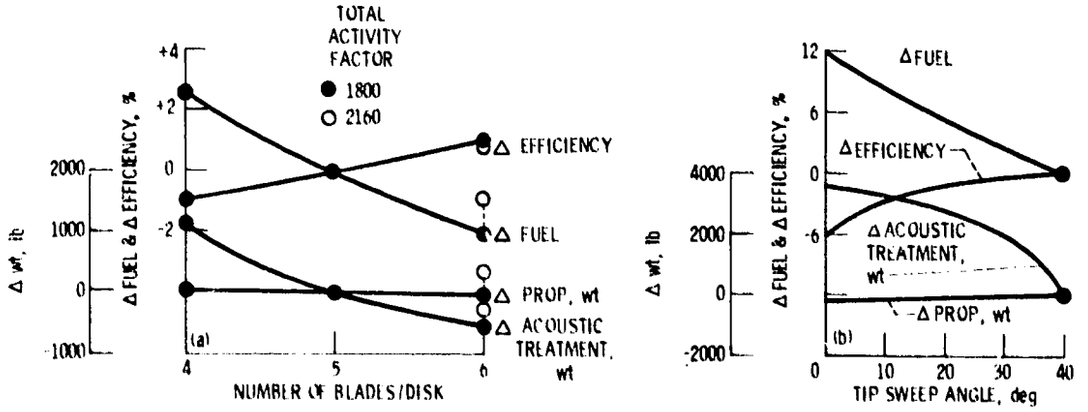

Figure 10. - Counter rotation propeller geometry optimization.

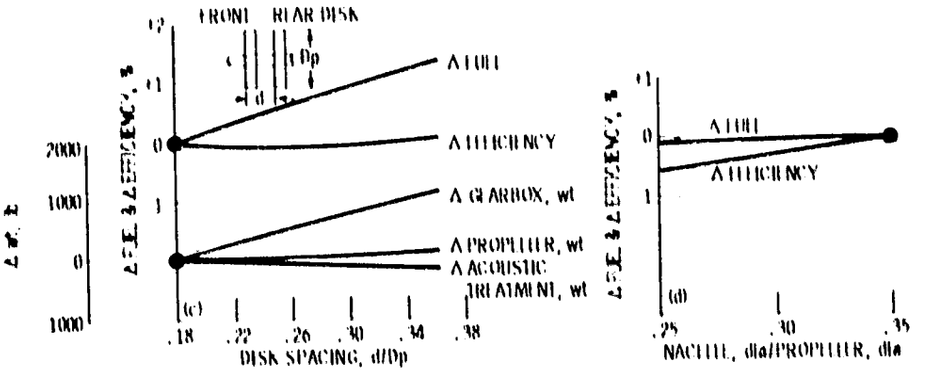

Figure 10.—Continued.

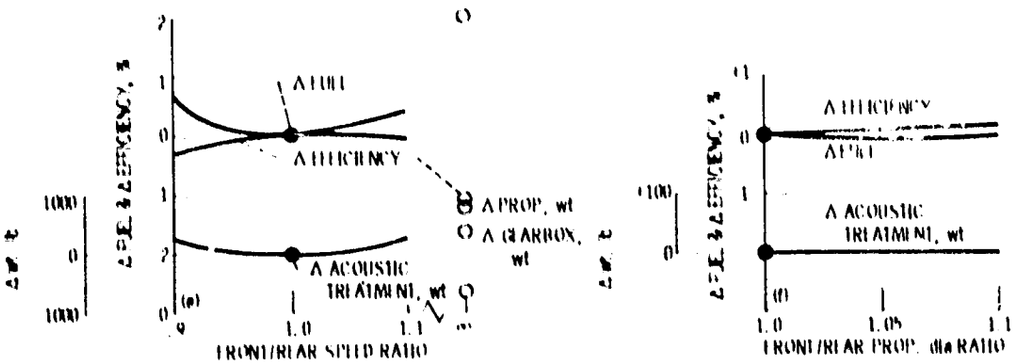

Figure 10.—Concluded.

NUMBER OF BLADES	12 (6x6)
ACTIVITY FACTOR	180
INTEGRATED DESIGN C_L	.31
TIP SWEEP, F &R	40^0 AFT
DISC SPACING/PROP DIA.	.18
NACELLE DIA./PROP DIA.	.25
DIAMETER RATIO, F/R	1.0
TIP SPEED RATIO, F/R	1.0
POWER SPLIT, F/R	55/45
POWER LOADING, SHP/D^2	36.8 (CRUISE)
TIP SPEED, ft/sec	750
CRUISE EFFICIENCY, %	89.1

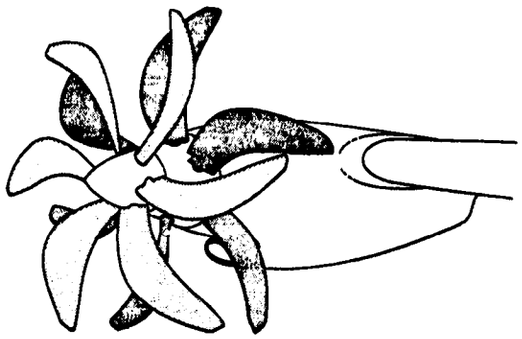

Figure 11. - Recommended counter rotation propeller configuration.

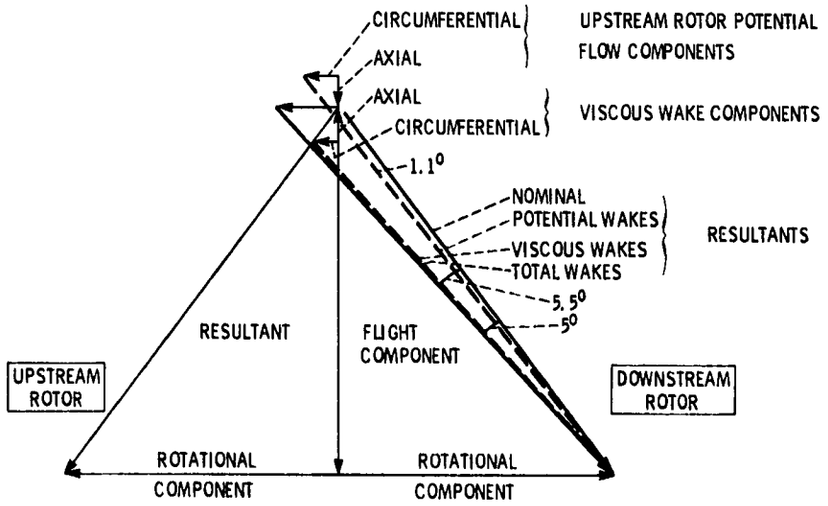

Figure 12. - Counter rotation propeller velocity diagram at 85% radius. Mach 0.8, 35000 ft cruise with 700 ft/sec tip speed.

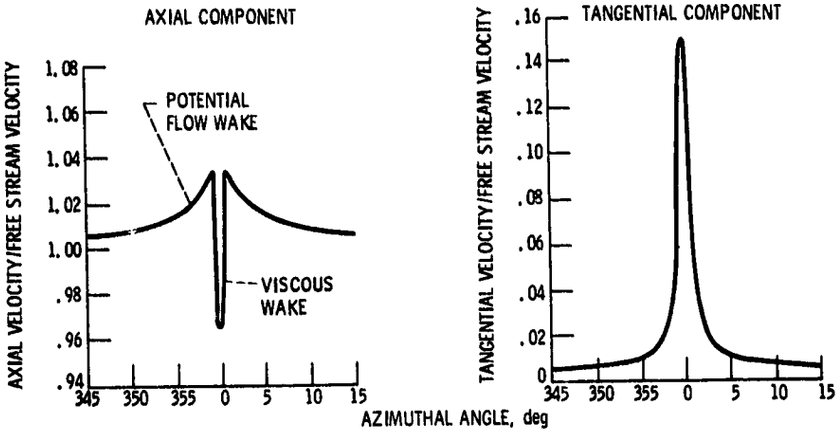

Figure 13. - Wake from one upstream rotor blade.

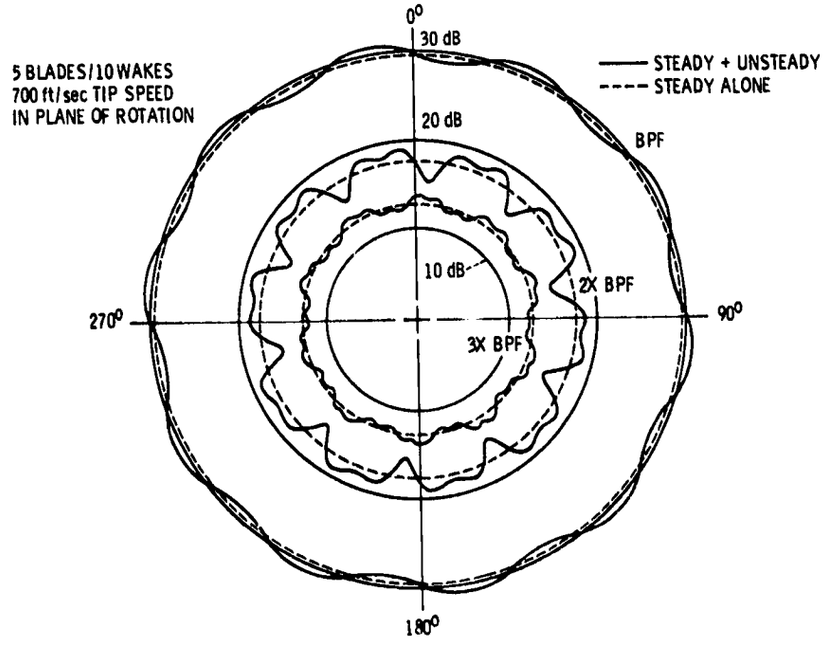

Figure 14. - CR rear rotor loading noise directivity.

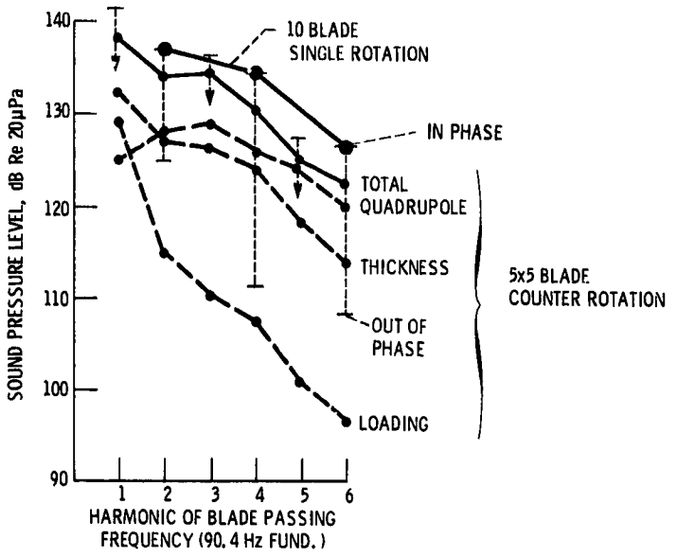

Figure 15. - Near-field noise components (tip speed = 700 ft sec; SHP/D^2 SHP/D^2 = 32; M 0.8 cruise at 35000 ft).

180.8 Hz HARMONIC	EXTERIOR SIDEWALL SPL	SIDEWALL ATTENUATION		SIDEWALL ATTENUATION	EXTERIOR SIDEWALL SPL	HARMONIC 90.4 Hz
1	137 dB	45 dB		34 dB	138.6 dB	1
				45	134.5	2
2	134.1	51		48.5	134.7	3
				51	131.2	4
				53	124.5	5
3	126.6	54.5		54.5	118.3	6

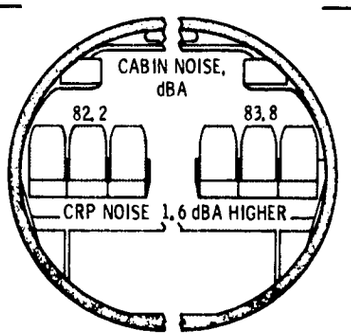

Figure 16. - Propeller induced cabin noise. Mach 0.8, 35000 ft cruise, 100 pass. twin engine airplane.

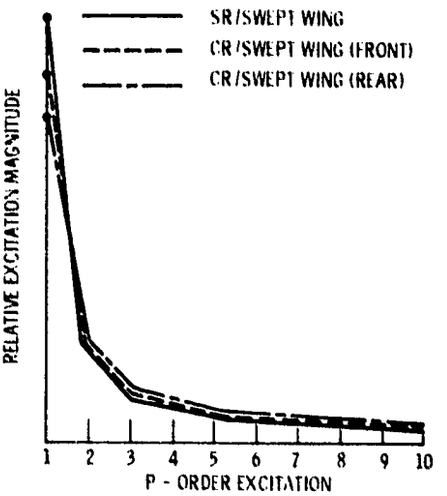

Figure 17. - Aerodynamic excitation of counter rotation prop-fan.

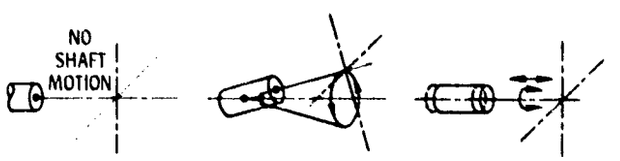

MODES	REACTIONLESS (R)	WHIRL	SYMMETRICAL
P - ORDER	SRP 12-WAY	CRP 6x6	WITH PROPER PHASING AND SYNCHROPHASING
1	F & M	FORCE ONLY	
2	R	R	
3	R	R	
4	R	R	
5	R	+ WHIRL	L
6	R	SYMM	R
7	R	- WHIRL	L
8	R	R	
9	R	R	
10	R	R	
11	+ WHIRL	+ WHIRL	L
12	SYMM	SYMM	R
13	- WHIRL	- WHIRL	L

L = LINEAR MOTION

WHIRL = IN-PLANE FORCE & OUT-OF-PLANE MOMENT

SYMM = OUT-OF-PLANE FORCE & IN-PLANE MOMENT

Figure 18. - Shaft reactions for propeller modes.

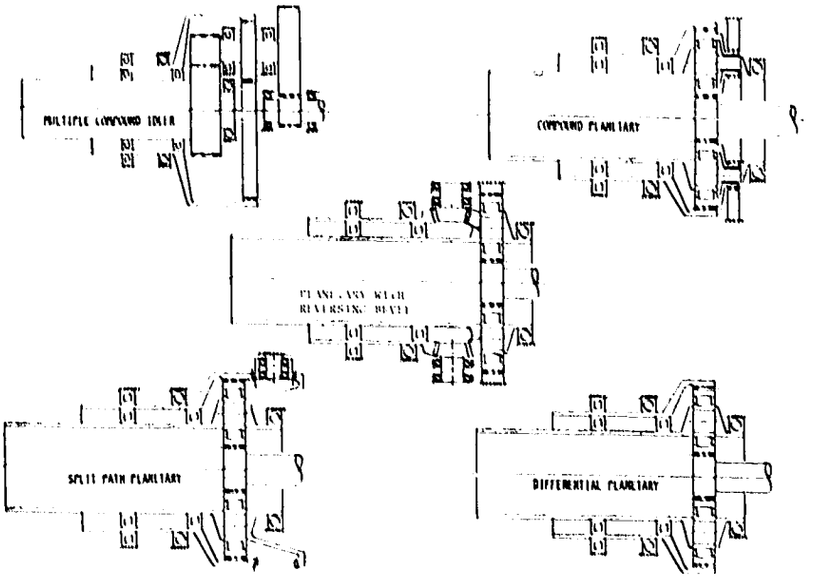

Figure 19. - In-line counter rotation gearbox candidates.

Figure 20. - Offset counter rotation gearbox candidates.

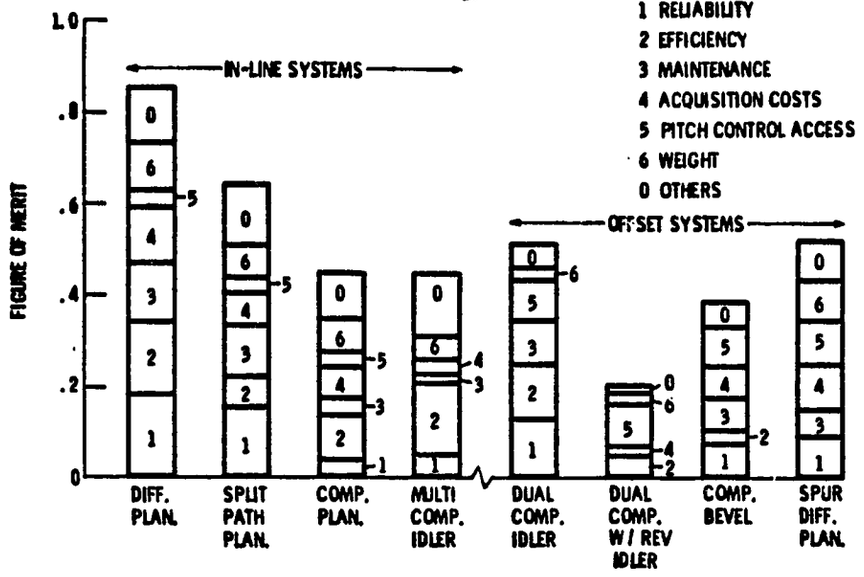

Figure 21. - Counter rotation gearbox figure of merit.

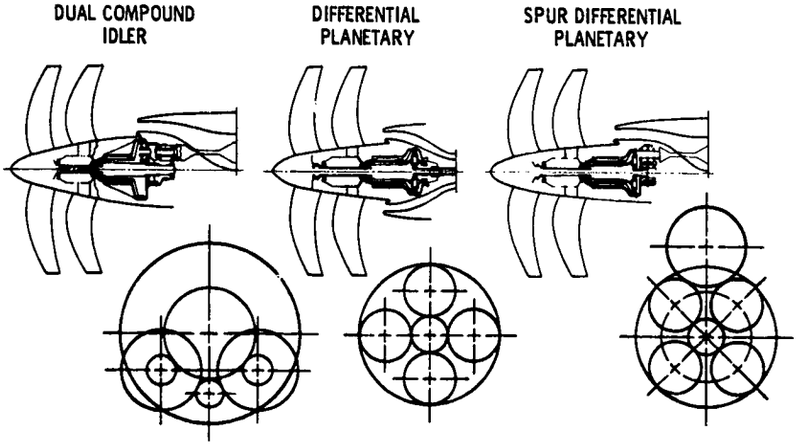

NO. OF GEARS/BEARINGS	9/13	6/11	8/12
MTBR, hr	24000	18000	21000
EFFICIENCY, %	BASE	+.3	-.4
WEIGHT	BASE	-37%	-30%
ACQUISITION COST	BASE	-9%	+4%
MAINTENANCE COST	BASE	-24%	-9%
MISSION FUEL	BASE	-1.6%	-.5%
DOC	BASE	-.9%	-.4%

Figure 22. - Counter rotation gearbox assessment.

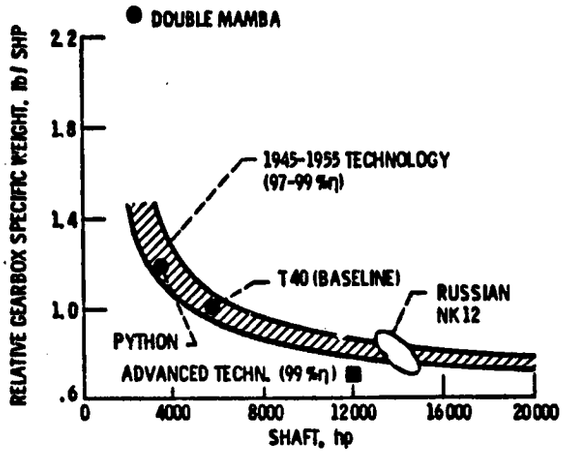

Figure 23. - Comparison of gearbox weights.

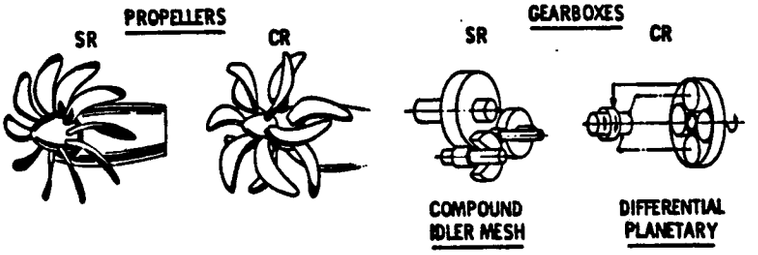

EFFICIENCY	BASE	+ 8 PTS	BASE	+0.2 PTS
WEIGHT	BASE	+ 17%	BASE	- 15%
ACQUISITION COST	BASE	+ 27%	BASE	+ 19%
MAINTENANCE COST	BASE	+ 34%	BASE	+ 8%
MTBR, hr	10 500	5900	33000	18000
SHP/D^2	BASE	+ 15%		
V_{TIP}, ft/sec	800	750		
DIAM, ft	BASE	- 1		
NO. OF BLADES	10	6x6		

Figure 24. - Comparison of 12000 SHP single and counter rotation systems.

COUNTER ROTATION AIRPLANE BENEFITS

100 PASSENGER, TWIN-ENGINE, MACH 0.8, 35000 ft, 1300 N.M. DESIGN

82 dBA CABIN NOISE, FAR 36-STAGE III FUEL, $1.50/gal

(400 N.M. TYP. - 60 PASS.)

	SINGLE ROTATION	COUNTER ROTATION
		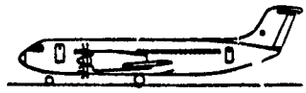
OWE - lb	55756	+.37%
TOGW - lb	75666	-.65%
SHP	1.120	- 2.1%
BLOCK FUEL, lb	3373	- 8.1%
DOC ¢/ASNM	11.82	- 2.5%

Figure 25. - Counter rotation airplane benefits.